Production of Focused Neutron Beam Using Heavy Ion Reaction

I. 20 Production of Focused Neutron Beam Using Heavy Ion Reaction

Hasegawa K., Seki H., Kotajima K., Kitamura M., Yamaya T.*, Satoh O.*,
Shinozuka T.** and Fujioka M.**
Department of Nuclear Engineering, Faculty of Engineering, Tohoku University
Department of Physics, Faculty of Science, Tohoku University*
Cyclotron and Radioisotope Center, Tohoku University**

Accurate measurements of the secondary neutrons originated from neutron-induced reactions or scatterings are usually disturbed severely by the source neutrons themselves. Because they are emitted more or less in every direction, and then scattered back from all quarters. Consequently, the experimental area (locations of the measuring sample and the neutron detector) is fully loaded with these stray neutrons. This situation is the root of all embarrassing backgrounds in neutron interaction measurements. Providing a heavy detector shield against these neutrons is sometimes quite effective, but not satisfactory for excluding the effects of the background neutrons. The essential way to eliminate the stray neutron disturbance, in principle, is to generate source neutrons into a very small forward cone (see Fig. 1). If such a focused neutron beam is produced, the uninteracted source neutrons after transmitting through the sample could easily be led to a neutron dump prepared in the far distance. The neutron detector, in this case, will look only at the neutrons coming from the sample. The use of the focused neutron beam could, therefore, make a great stride in improving the accuracy of the neutron interaction measurements, just as we can observe stars more clearly at night than in day time. In this sense, we have studied the feasibility of producing a monoenergetic neutron beam using the Tohoku University K=50 AVF Cyclotron.[1)]

Practically, there are two ways of producing such a focused neutron beam by the heavy ion reaction of ^{1}H(HI,n) type, as illustrated in Fig. 2. The velocity of generated neutron in the laboratory system V_L is the vector sum of the neutron velocity in the center-of-mass system V_n and the velocity of the centroid V_G . The first method so-called "momentum-focusing" is to take V_G as large as possible compared to V_n . When the projectile heavy ion energy (therefore, V_G also) is increased by a considerable amount, the excess energy will act mostly to increase the number of emitted nucleons, and their average energy (therefore, V_n also) stays rather constant. Therefore, the resultant V_L points more to the forward direction. Since V_n in this case is not definite, the maximum emission angle of the neutrons in the laboratory system θ_{max} can not be defined. The disadvantage of this method is that a very high-energy heavy ion accelerator (probably $\sim$100 MeV/A or more) is required. The second method so-called "kinematic focusing" is to make V_n as small as possible compared to V_G , so that the resultant V_L points to the forward

angle. To realize this, the projectile heavy ion energy E_{proj} should be taken slightly above the threshold energy E_{th} of the endoenergetic reaction. Then the excess energy converted to V_n bocomes very small. Based on this method, an experiment to produce neutron beam had been reported.[2] Since the V_n in this case is unique, the maximum emission angle of the neutrons in the laboratory system θ_{max} is given by

$$\theta_{max} = \sin^{-1}(V_n/V_G)$$
$$= \sin^{-1}(1-E_{th}/E_{proj})^{1/2}. \quad (1)$$

The advantage of this method is that the required bombarding energy of the heavy ion is much lower than that in the case of momentum focusing, and thus, any presently operating heavy ion cyclotron can be used immediately. Moreover, the associated gamma-ray yield is expected to be extremely small compared to that for a conventional neutron target. These are the reasons of using kinematic focusing in the present study. Table 1 shows a list of endoenergetic heavy ion reactions on hydrogen target for the production of a monoenergetic focused neutron beam by the kinematic focusing. In the present work, the $^{1}H(^{13}C,n)^{13}N$ reaction was used taking into account the available heavy ion species and acceleration energies[3] of the cyclotron.

The experimental setup for measuring the energy spectra, angular distributions and production yields of the focused neutrons is schematically shown in Fig. 3. The accelerated $^{13}C^{4+}$ ion beam was led through 0.3-cmϕ Ta double collimators onto a 1.2 cmϕ × 3.0 cm hydrogen gas cell with a 7.5-μm thick Ta foil as the beam entrance window. A 0.1-mm thick Pt plate was used as the beam stopper. The gas pressure was 0.5 atm, and was monitored with a semiconductor type pressure transducer of 0.5 % accuracy. The energy losses of the 57.7-MeV ^{13}C beam in the Ta window and H_2 gas were estimated to be 14.6 MeV and 1.13 MeV, respectively, using the tabulation by Northcliffe and Schilling.[4] From their figures, the actual bombarding energy was estimated to be 42.5 MeV. The whole gas cell assembly was electrically insulated from the ground to measure the $^{13}C^{4+}$ beam current. A 2"ϕ × 2" NE213 liquid scintillation neutron detector was mounted at the distance of 60-180 cm on a stand which could be moved along the concentric circumference of a circle centered at the gas cell position. The neutron energy spectra were measured by time-of-flight using the beam chopping signals as the stop pulses. The NE213 detector signals were fed to the PDP-11/44 computer for the analysis. A 70-cc Ge(Li) detector was fixed at 60 cm from the gas cell to evaluate the associated gamma-ray yield.

Neutron energy spectra of the $^{1}H(^{13}C,n)^{13}N$ reaction measured by time-of-flight are shown as a function of the emission angle θ in Fig. 4 for the bombarding energies of 45.0 MeV (above) and 42.5 MeV (below). At 45.0 MeV, two neutron components (4.2 and 1.9 MeV at 0°), each corresponding to the

forward and backward emissions in the center-of-mass system, were observed. As the emission angle becomes larger, the energy difference between the two compoenents becomes smaller (see also Fig. 5). At 42.5 MeV, the only one component (2.7 MeV at 0°) was observed. As the emission angle becomes larger, this component disappears very rapidly. These behaviors are exactly what we expect from the endoenergetic heavy ion reaction kinematics as shown graphically in Fig. 5.

Angular distributions of the generated neutrons are shown in Fig. 6 for the bombarding energies of 45.0 MeV (left) and 42.5 MeV (right). When the bombarding energy became close to the reaction threshold, the angular distribution of the neutrons (the maximum emission angle θ_{max}) turned out to be somewhat unstable. This is explained by the fact that the sensitivity of θ_{max} to the bombarding energy can be expressed as

$$d\theta_{max}/dE_{proj} = 1/(2E_{proj}\sqrt{(E_{proj}/E_{th})-1}) \qquad (2)$$

by differentiating the Eq. (1). Thus, for producing a stable focused neutron beam with a cyclotron, the stabilization of the bombarding energy as well as the beam intensity should be attained.

The measured neutron yield was $\sim 10^4$ n/10 enA for the bombarding energy of 45.0 MeV. This gives a value of $\sim$5 mb for the corresponding total cross section of the $^{1}H(^{13}C,n)^{13}N$ reaction. The beam current of the accelerated $^{13}C^{4+}$ ions at the extraction radius (R = 65.0 cm) of the cyclotron was $\sim$1 eμA[5], which indicates a good possibility of producing a focused neutron beam of $\sim 10^6$ n/sec.

In order to evaluate the gamma-ray background associated with this neutron producing process, the gamma-ray spectra were measured with a 70-cc Ge(Li) detector (see Fig. 3) for the following cases.

A) Natural background was measured without ^{13}C ion beam.
B) Background due to the 60-MeV incident ^{13}C ion beam was measured with the empty gas cell.
C) Background due to the neutron production was measured with the 60-MeV incident ^{13}C ion beam onto the hydrogen filled gas cell.

The obtained spectra are shown in Fig. 7. In the spectrum (A), all the observed gamma-ray peaks are identified to be due to the decay of natural activities such as ^{40}K, ^{208}Tl, $^{211,214}Pb$, ^{214}Bi and ^{228}Ac, and due to the decay of induced activities such as ^{54}Mn and $^{56,58}Co$ in the surrounding materials. Besides these activities, gamma rays due to the Coulomb excitation of Ta were recognized in the spectra (B) and (C). It is clear from the Fig. 7 that the spectra (B) and (C) are almost identical. This indicates a fact that there is practically no gamma-ray background associated with the focused neutron beam.

As described above, a monoenergetic focused neutron beam of 2.8 MeV with

a flux of $\sim 10^4$ n/sec was produced by bombarding the hydrogen gas cell with a $^{13}C^{4+}$ ion beam of $\sim$10 enA. When an internal irradiation of the target in the cyclotron can be done, we can expect a neutron flux of $\sim 10^6$ n/sec or more. This figure is still somewhat small for an application of the present method to neutron dosimetry or neutron therapy. However, it should be noted that the focused neutron beam of this type has almost no associated neutron or gamma-ray backgrounds. Therefore, it is very suitable to apply this method for calibrating the detection efficiency of neutron detectors with a higher precision, which could considerably improve the present accuracy of the neutron interaction measurements.

References

1) Morita S., Fujioka M., Orihara H., Tazawa S., Yoshimura C., Fujii K., Takayama T., Maruyama M., Abe J., Mita T. and Yamamoto M., IEEE Trans. Nucl. Sci. NS-26 (1979) 1930.
2) Dave J. H., Gould C. R., Wender S. A. and Shafroth S. M., Nucl. Instr. and Meth. 200 (1982) 285.
3) Yamaya T., Shinozuka T., Kotajima K., Fujioka M. and Onodera T., Nucl. Instr. and Meth. 226 (1984) 219.
4) Northcliffe L. C. and Schilling R. F., Nucl. Data Table A7 (1970) 233.
5) Fujioka M., Shinozuka T., Sera K., Orihara H., Ishii K. and Ido T., 11th Int. Conf. on Cyclotrons and Their Appl. D42, Tokyo, 1986.

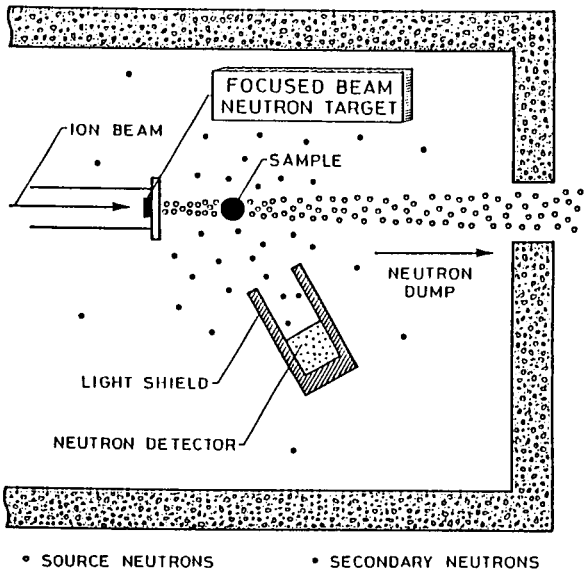

Fig. 1. Conceptional drawing of the low-background secondary neutron measuring system using a focused neutron beam.

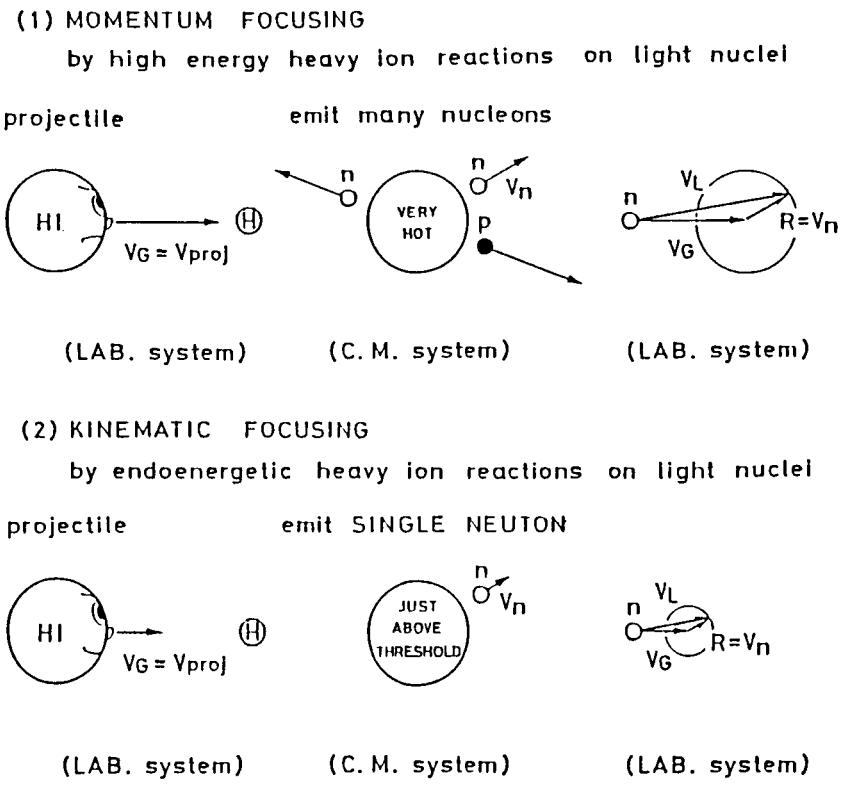

Fig. 2. Illustrations of producing the focused neutron beam by (1) MOMENTUM FOCUSING and by (2) KINEMATIC FOCUSING.

Table 1 Candidates for producing the monoenergetic focused neutron beam with ^{1}H target

projectiles	E_{th} (MeV)	E_n (MeV)	projectiles	E_{th} (MeV)	E_n (MeV)
^{7}Li	13.09	1.44	^{6}Li	35.35	4.35
^{9}Be	18.40	1.67	^{14}N	88.30	5.53
^{11}B	32.97	2.53		⋮	
^{13}C	41.75	2.79	^{12}C	234.1	16.7
^{19}F	79.82	3.82		⋮	
^{10}B	48.49	4.03			

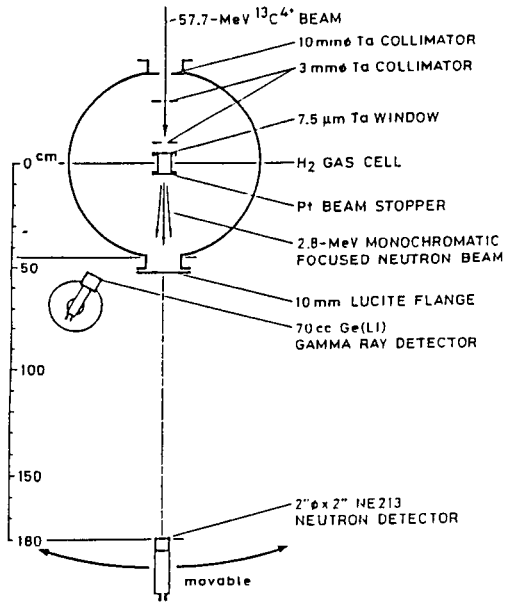

Fig. 3. Schematic drawing of the experimental setup to produce a monoenergetic focused neutron beam of 2.8 MeV by the $^{1}H(^{13}C,n)^{13}N$ reaction.

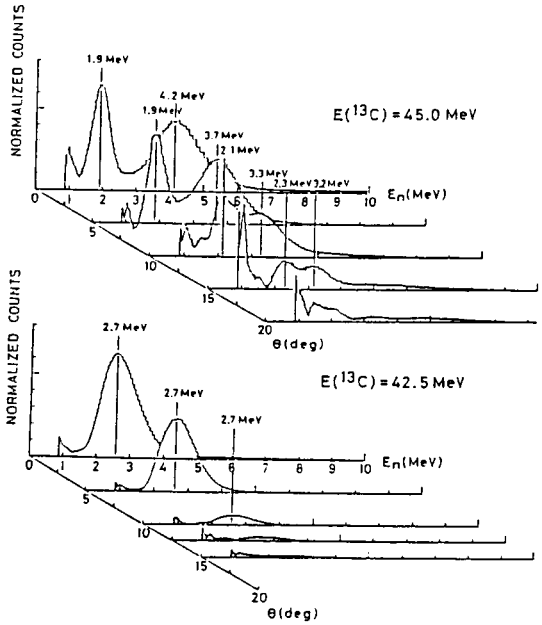

Fig. 4. Neutron energy spectra of the $^{1}H(^{13}C,n)^{13}N$ reaction measured by TOF for $E(^{13}C)$ = 45.0 MeV (above) and $E(^{13}C)$ = 42.5 MeV (below).

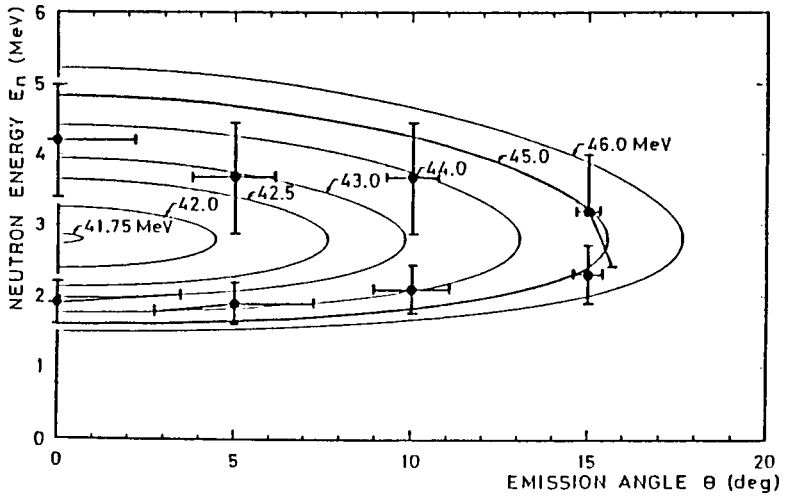

Fig. 5. Kinematics of the $^{1}H(^{13}C,n)^{13}N$ reaction near threshold taking the projectile energy as a parameter. The measured neutron energies vs. emission angle are also indicated for $E(^{13}C)$ = 45.0 MeV.

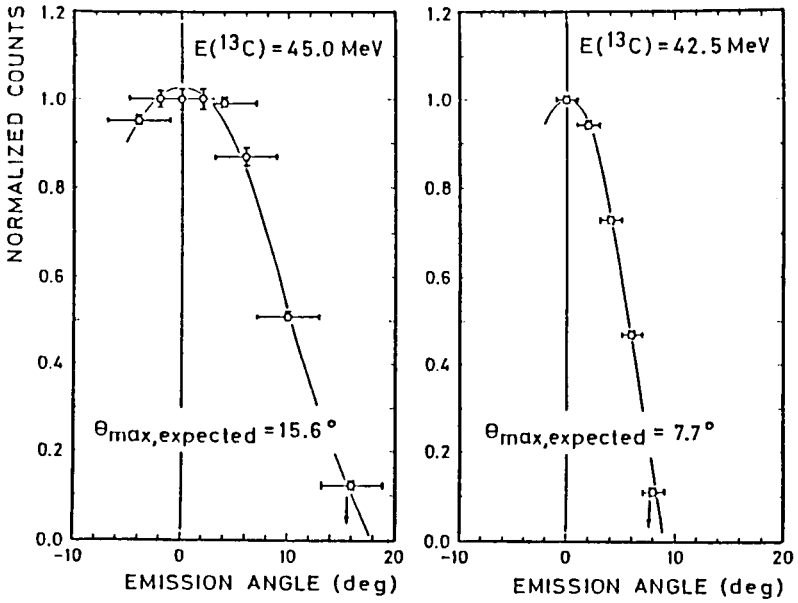

Fig. 6. Measured neutron angular distributions of the $^{1}H(^{13}C,n)^{13}N$ reaction for $E(^{13}C)$ = 45.0 MeV (left) and $E(^{13}C)$ = 42.5 MeV (right). The maximum emission angles of the generated neutrons θ_{max} estimated from the Eq. (1) are shown with arrows.

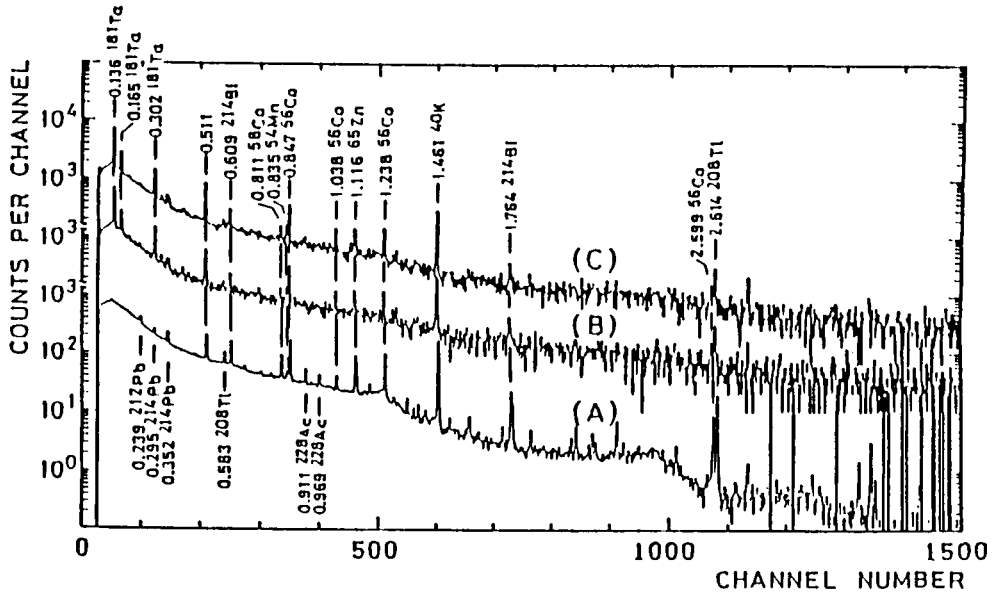

Fig. 7. Measured gamma-ray spectra with a 70-cc Ge(Li) detector mounted at 60 cm from the H_2 gas cell. Each corresponds to

(A) natural background spectrum,

(B) background spectrum of the gas cell without H_2 gas bombarded by the 60-MeV ^{13}C ion beam, and

(C) background spectrum of the gas cell filled with 0.5-atm H_2 gas bombarded by the 60-MeV ^{13}C ion beam.

The ordinate is shifted by an order for easy inspection.